

Research Journal of Pharmaceutical, Biological and Chemical Sciences

Structure Activity/Property Relationships of pyrazole Derivatives by MPO and QSAR Methods for Drug Design.

Riadh Hanachi¹, Salah Belaidi², Aicha Kerassa² and Salima Boughdiri^{1*}.

¹Research Unit: Physico-Chimie des Matériaux à l'état Condensé, Faculty of Sciences of Tunis, El Manar University, 2092-Tunis, Tunisia.

²Group of Computational and pharmaceutical Chemistry, LMCE Laboratory, Department of chemistry, Faculty of Sciences, University of Biskra, 07000, Biskra, Algeria.

ABSTRACT

Molecular geometry, electronic structure, effect of the substitution and structure/ Property / activity relationships for pyrazole derivatives, have been studied by molecular mechanics, PM3, DFT and QSAR methods. In the present work, calculated values, namely net charges, MESP contours/surfaces has also been drawn to explain the electronic activity of pyrazoles, bond lengths, electron-affinities, drug-likeness, LipE and QSAR properties, are reported and discussed in terms of the biological activity of pyrazole derivatives.

Keywords: pyrazole, MPO, FMOs, MEP, RO5, QSAR properties, lipE.

**Corresponding author*

INTRODUCTION

The idea that the physiological effects of a substance depend on its chemical composition and structure was first formulated more than a hundred years ago [1]. Today this approach is widely used in biochemical, pharmaceutical and other fields of science where predicting properties of chemical compounds is necessary. The popularity of this approach is based on the now obvious statement that the biological or physicochemical activity of the compound is a function of its structure, represented by a set of directly measurable or computable parameters [2-6]. Heterocyclic compounds hold a special place among the major pharmaceutical natural products and synthetic drugs having different biological activities [7]. Pyrazole derivatives are the subject of many research studies due to their widespread potential biological activities such as antimicrobial [8], antiviral [9], antitumor [10,11], antihistaminic [12], antidepressant [13], insecticides and fungicides [14].

A successful drug that passes the hurdles of clinical trials to gain approval and a strong market position must exhibit a delicate balance of biological and physicochemical properties [15,16].

A representative set of pyrazole derivatives was chosen from the series tested on 2011 for aVGF2R-2 activity [17]. Multi-parameter optimization (MPO) is used to select high quality compounds and describe the range of methods that have been employed in drug design, including; simple 'rules of thumb' such as Lipinski's rule [18-21].

This method has been applied to predicted and experimental data to reduce attrition and improve the productivity of the drug design process [22].

MATERIALS AND METHODS

All calculations were performed by using HyperChem 8.0.6 software [23], Gaussian 09 program package [24] and Molinspiration online database [25]. The geometries of pyrazoles and their methyl, cyanide derivatives were fully optimized by, MP3 and DFT/B3LYP with 6-31++G(d,p) basis by Gaussian 09 program package. The calculation of QSAR properties is performed by the module QSAR Properties, (version 8.0.6). QSAR Properties is a module, that together with HyperChem, allows several properties commonly used in QSAR studies to be calculated. Molinspiration, web based software was used to obtain parameter such as TPSA, HBA, HBD, nrotb and drug likeness.

RESULTS AND DISCUSSION

Geometric and Electronic Structure of pyrazole:

The optimized geometrical parameters of pyrazole (Figure 1) are obtained using DFT/B3LYP method, listed in [Table 1] with the experimental results [26-27] which are approximately similar to the theoretical results, regarding bond length and valence angle values. The theoretical dihedral angle values calculated by DFT method and basis are practically equal to zero degree which explain that the geometry of pyrazoles is planar, which makes this conformation more stable.

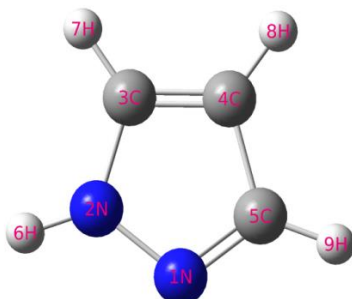


Figure 1: 3D structure of pyrazole

Table 1. Bond lengths and valence angles of pyrazole at DFT/B3LYP level.

	Parameters	Exp.	6-31+ (d,p)	6-31++(d,p)	6-311++ (d,p)	cc-pVTZ
Bond length (angstrom)	N1-N2	1.351	1.351	1.350	1.348	1.344
	N1-C5	1.332	1.334	1.333	1.330	1.327
	C4-C5	1.417	1.416	1.416	1.414	1.410
	C3-C4	1.374	1.383	1.383	1.380	1.376
	C3-N2	1.360	1.360	1.360	1.358	1.354
	N2-H	1.002	1.008	1.008	1.007	1.004
	C5-H	1.083	1.081	1.081	1.080	1.077
	C4-H	1.080	1.080	1.079	1.078	1.075
	C3-H	1.082	1.080	1.080	1.078	1.076
Valence angle (degree)	C3-N2-N1	113.0	113.2	113.2	113.1	113.1
	C4-C3-N2	106.4	106.2	106.2	106.1	106.2
	C5-C4-C3	104.5	104.5	104.5	104.6	104.5
	N2-N1-C5	104.1	104.2	104.2	104.3	104.2
	H-N2-N1	118.4	118.2	118.9	119.0	119.1
	H-C3-N2	121.4	121.2	121.9	122.0	122.0
	H-C4-C3	127.6	127.3	127.3	127.3	127.3
	H-C4-C5	128.8	128.2	128.2	128.1	128.2

Mulliken population analysis and natural population analysis of pyrazole:

The effective atomic charges calculation which depicts the charges of the every atom in the molecule distribution of positive and negative charges are vital to increase or decrease in bond length between the atoms. Atomic charges, dipole moment, molecular polarizability, electronic structure, acidity–basicity behavior and lot of properties of molecular system and electrostatic potential surfaces [28-31].

The total atomic charges of the Mulliken population analysis and the natural population analysis (NPA) are listed in [Table 2].

Table 2: Calculated net charges by Mulliken population method and natural population analysis (NPA).

atoms	B3LYP/6-31++G(d,p) Mulliken charges	B3LYP/6-31++G (d,p) (NPA) Natural charges
N 1	-0.187	-0.299
N2	-0.173	-0.376
C3	-0.227	-0.604
C4	0.067	-0.360
C5	-0.209	-0.065

Mulliken population analysis and NPA are obtained from optimized geometry and NBO [32] results, respectively. The two methods predict the same tendencies except for C4 atom (figure 2).

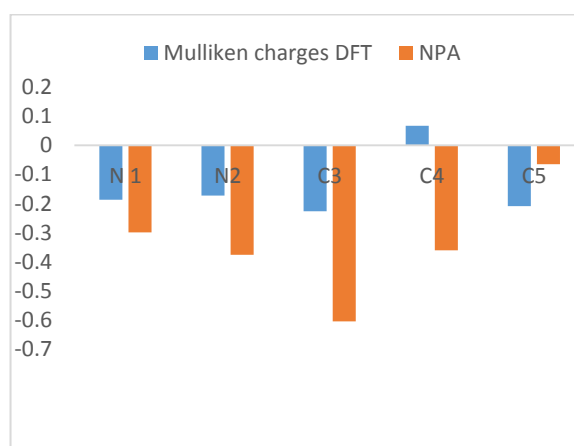


Figure 2: Mulliken and Natural charges of pyrazole

Molecular Electrostatic Potential (MEP) surface of pyrazole:

The molecular electrostatic potential (MESP) surface, which is a plot of electrostatic potential mapped onto the iso-electron density surface [33], the importance of the MESP lies in the fact that it simultaneously displays the molecular size and shape as well as positive, negative and neutral electrostatic potential regions in terms of the electrostatic surface, which explain the investigation of the molecular structure with its physiochemical property relationships [34,35]. The MESP surface map and contour map of pyrazole (Figure 3) show one region characterized by red color (negative electrostatic potential) around one cyclic nitrogen atom (N1) which explain the ability for an electrophilic attack on this position, also by blue color (positive electrostatic potential) around the four hydrogen atoms which explain that these regions are susceptible for a nucleophilic attack.

Finally for the green color located between the red and blue regions explain the neutral electrostatic potential surface.

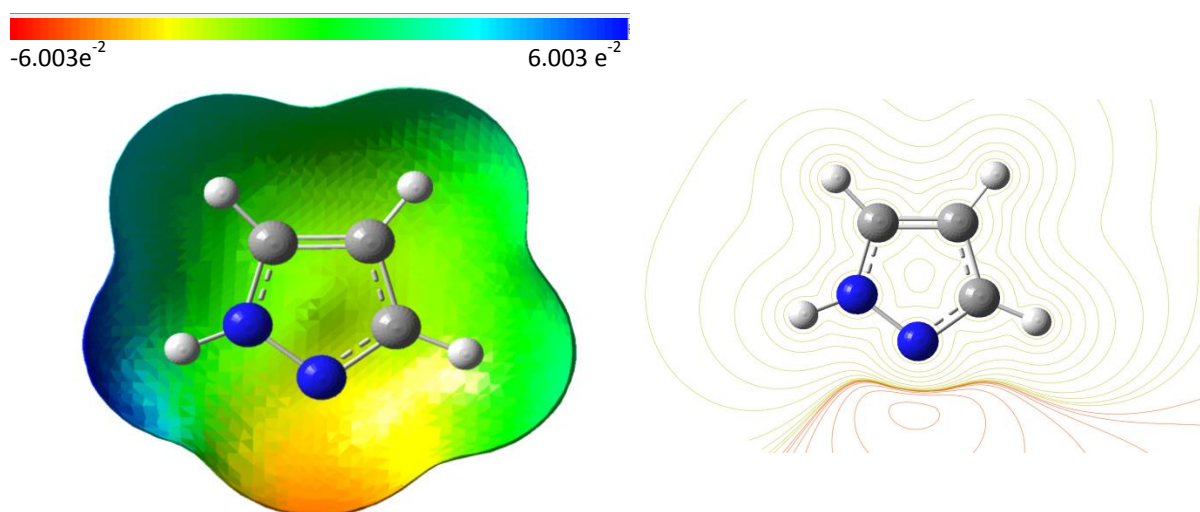


Figure 3: 3D MESP surface map and 2D MESP contour map for pyrazole

The variation in electrostatic potential produced by a molecule is largely responsible for binding of a drug to its active sites (receptor), as the binding site in general is expected to have opposite areas of electrostatic potential [36].

The Substitution Effect on Pyrazole Structure:

The Frontier orbitals, highest occupied molecular orbital (HOMO) and lowest unoccupied molecular orbital (LUMO) are important factors in quantum chemistry [37] as these determine the way the molecule interacts with other species. The frontier orbital gap helps characterize the chemical reactivity and kinetic stability of the molecule. A molecule with a small frontier orbital gap is more polarizable and is generally associated with a high chemical reactivity, low kinetic stability and is also termed as soft molecule [38].

For understanding various aspects of pharmacological sciences including drug design and the possible eco-toxicological characteristics of the drug molecules, several new chemical reactivity descriptors have been proposed. Conceptual DFT based descriptors have helped in many ways to understand the structure of the molecules and their reactivity by calculating the chemical potential, global hardness and electrophilicity. Using HOMO and LUMO orbital energies, the ionization energy and electron affinity can be expressed as: $I = -E_{\text{HOMO}}$, $A = -E_{\text{LUMO}}$, $\eta = (-E_{\text{HOMO}} + E_{\text{LUMO}})/2$ and $\mu = (E_{\text{HOMO}} + E_{\text{LUMO}})/2$ [39]. Parr et al, [40] proposed the global electrophilicity power of a ligand as $\omega = \mu^2/2\eta$.

This index measures the stabilization in energy when the system acquired an additional electronic charge from the environment. Electrophilicity encompasses both the ability of an electrophile to acquire additional electronic charge and the resistance of the system to exchange electronic charge with the

environment. It contains information about both electron transfer (chemical potential) and stability (hardness) and is a better descriptor of global chemical reactivity. The hardness η and chemical potential μ are given by the following relations: $\eta = (I-A)/2$ and $\mu = -(I+A)/2$, where I and A are the first ionization potential and electron affinity of the chemical species [41].

The calculated values of (methyl, Cyanide) substituted Pyrazole (Figure 4) are given in [Table 3].

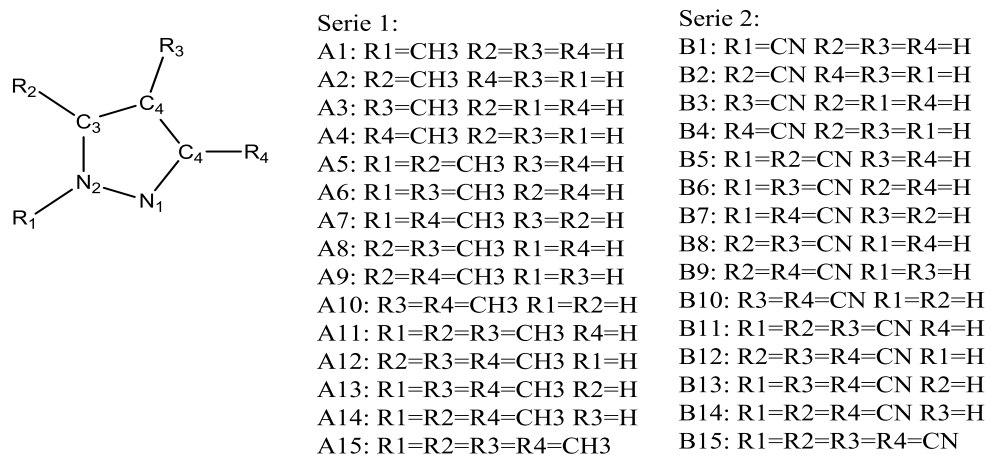


Figure 4: pyrazole systems

In [Table 3] has been seen by calculating the effect of a substituent donor (CH₃) and a substituent acceptor (CN).

We note from the [Table 3] that the compound 11 (1,4,5-trimethyl-4,5-dihydro-1H-pyrazole) and compound 15 (1,3,4,5-tetramethyl-4,5-dihydro-1H-pyrazole) have smaller HOMO - LUMO energy gap (5.17 eV) than others, thus, these compounds are the most reactive. We can note also that compound 15 has higher ionization energy (I) (9.25eV), higher electron affinity (A) (4.08eV), smaller global hardness (η) (2.58eV), higher global softness (S) (0.19eV), and higher global electrophilicity index (Ω) (8.60eV) thus, compound 15 is a strong electrophile than others compounds. And we can see that all values of chemical potential of all compounds are negative and it means that the compounds are stable.

In the same way, the high value of chemical potential (3.13eV) and low value of electrophilicity index (1.71eV) for compound B15 favor its nucleophilic behavior.

It can be seen from the plots of compound A15 that the HOMO levels are spread over the entire molecule except the carbone of cyanide and all positive and negative phase are distributed symmetrical. The LUMO is almost distributed over the molecule without cyanide group, and all positive and negative phase are distributed symmetrically but the LUMO reflects a lot of antibonding π^* character as compared to HOMO.

While, for compound A11 the HOMO levels are spread over the entire molecule except the carbone of cyanide and all positive and negative phase are distributed symmetrical.

The LUMO is almost distributed over the molecule without CH group of pyrazole cycle, and all positive and negative phase are distributed symmetrically but the HOMO reflects a lot of antibonding π^* character as compared to LUMO.

Table 3. Calculated E_{HOMO} , E_{LUMO} , energy band gap (ΔE), ionization energy (I), electronegativity(A), global hardness (η), global softness (S) and global electrophilicity index (Ω)

Comp.	Systems	E_{HOMO} (ev)	E_{LUMO} (ev)	ΔE (ev)	μ (D)	I (ev)	A (ev)	S (ev^{-1})	μ (ev)	η (ev)	Ω (ev)
P	4,5-dihydro-1H-pyrazole	-7.08	-0.27	6.80	2.40	7.08	0.27	0.15	-3.67	3.40	1.98
A1	1-methyl-4,5-dihydro-1H-pyrazole	-7.89	-1.63	6.26	2.51	7.89	1.63	0.16	-4.76	3.13	3.62
A2	5-methyl-4,5-dihydro-1H-pyrazole	-7.62	-1.63	5.99	2.95	7.62	1.63	0.17	-4.63	2.99	3.57
A3	4-methyl-4,5-dihydro-1H-pyrazole	-7.62	-1.09	6.53	2.5	7.62	1.09	0.15	-4.35	3.26	2.90
A4	3-methyl-4,5-dihydro-1H-pyrazole	-7.89	-1.36	6.53	2.00	7.89	1.36	0.15	-4.63	3.26	3.28
A5	1,5-dimethyl-4,5-dihydro-1H-pyrazole	-8.44	-2.99	5.44	2.98	8.44	2.99	0.18	-5.71	2.72	6.00
A6	1,4-dimethyl-4,5-dihydro-1H-pyrazole	-8.44	-2.45	5.99	2.53	8.44	2.45	0.17	-5.44	2.99	4.95
A7	1,3-dimethyl-4,5-dihydro-1H-pyrazole	-8.44	-2.45	5.99	2.10	8.44	2.45	0.17	-5.44	2.99	4.95
A8	4,5-dimethyl-4,5-dihydro-1H-pyrazole	-8.16	-2.72	5.44	2.98	8.16	2.72	0.18	-5.44	2.72	5.44
A9	3,5-dimethyl-4,5-dihydro-1H-pyrazole	-8.44	-2.45	5.99	2.58	8.44	2.45	0.17	-5.44	2.99	4.95
A10	3,4-dimethyl-4,5-dihydro-1H-pyrazole	-8.16	-1.90	6.26	2.11	8.16	1.90	0.16	-5.03	3.13	4.05
A11	1,4,5-trimethyl-4,5-dihydro-1H-pyrazole	-8.98	-3.81	5.17	2.88	8.98	3.81	0.19	-6.39	2.58	7.91
A12	3,4,5-trimethyl-4,5-dihydro-1H-pyrazole	-8.71	-3.27	5.44	2.58	8.71	3.26	0.18	-5.99	2.72	6.58
A13	1,3,4-trimethyl-4,5-dihydro-1H-pyrazole	-8.98	-3.27	5.71	2.05	8.98	3.26	0.17	-6.12	2.86	6.56
A14	1,3,5-trimethyl-4,5-dihydro-1H-pyrazole	-8.98	-3.54	5.44	2.54	8.98	3.54	0.18	-6.26	2.72	7.20
A15	1,3,4,5-tetramethyl-4,5-dihydro-1H-pyrazole	-9.25	-4.08	5.17	2.52	9.25	4.08	0.19	-6.67	2.58	8.60
B1	4,5-dihydro-1H-pyrazole-1-carbonitrile	-6.80	-0.27	6.53	4.82	6.80	0.27	0.15	-3.54	3.26	1.92
B2	4,5-dihydro-1H-pyrazole-5-carbonitrile	-6.53	-0.54	5.99	2.14	6.53	0.54	0.17	-3.54	2.99	2.09
B3	4,5-dihydro-1H-pyrazole-4-carbonitrile	-6.53	-0.27	6.26	4.76	6.53	0.27	0.16	-3.40	3.13	1.85
B4	4,5-dihydro-1H-pyrazole-3-carbonitrile	-6.80	-0.27	6.53	6.66	6.80	0.27	0.15	-3.54	3.26	1.92
B5	4,5-dihydro-1H-pyrazole-1,5-dicarbonitrile	-6.53	-0.27	6.26	5.46	6.53	0.27	0.16	-3.40	3.13	1.85
B6	4,5-dihydro-1H-pyrazole-1,4-dicarbonitrile	-6.53	-0.27	6.26	0.22	6.53	0.27	0.16	-3.40	3.13	1.85
B7	4,5-dihydro-1H-pyrazole-1,3-dicarbonitrile	-6.53	-0.27	6.26	4.97	6.53	0.27	0.16	-3.40	3.13	1.85
B8	4,5-dihydro-1H-pyrazole-4,5-dicarbonitrile	-6.26	-0.54	5.71	4.67	6.26	0.54	0.17	-3.40	2.86	2.02
B9	4,5-dihydro-1H-pyrazole-3,5-dicarbonitrile	-6.53	-0.27	6.26	2.56	6.53	0.27	0.16	-3.40	3.13	1.85
B10	4,5-dihydro-1H-pyrazole-3,4-dicarbonitrile	-6.53	-0.27	6.26	7.85	6.53	0.27	0.16	-3.40	3.13	1.85
B11	4,5-dihydro-1H-pyrazole-1,4,5-tricarbonitrile	-6.26	-0.54	5.71	3.44	6.26	0.54	0.17	-3.40	2.86	2.02
B12	4,5-dihydro-1H-pyrazole-3,4,5-tricarbonitrile	-6.26	-0.27	5.99	5.45	6.26	0.27	0.17	-3.26	2.99	1.78
B13	4,5-dihydro-1H-pyrazole-1,3,4-tricarbonitrile	-6.26	-0.27	5.99	3.61	6.26	0.27	0.17	-3.26	2.99	1.78
B14	4,5-dihydro-1H-pyrazole-1,3,5-tricarbonitrile	-6.53	-0.54	5.99	2.37	6.53	0.54	0.17	-3.54	2.99	2.09
B15	4,5-dihydro-1H-pyrazole-1,3,4,5-tetracarbonitrile	-5.99	-0.27	5.71	1.29	5.99	0.27	0.17	-3.13	2.86	1.71

$$\Delta E = E_{\text{HOMO}} - E_{\text{LUMO}}$$

The low value of chemical potential (-6.67eV) and high value of electrophilicity index (8.60eV) for compound A15 favor its electrophilic behavior.

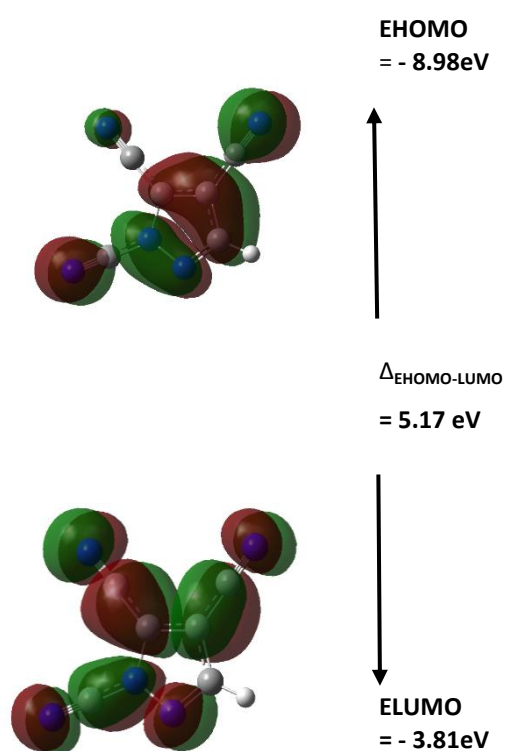


Figure 5: Schematic drawings of the HOMO and LUMO of compound A11

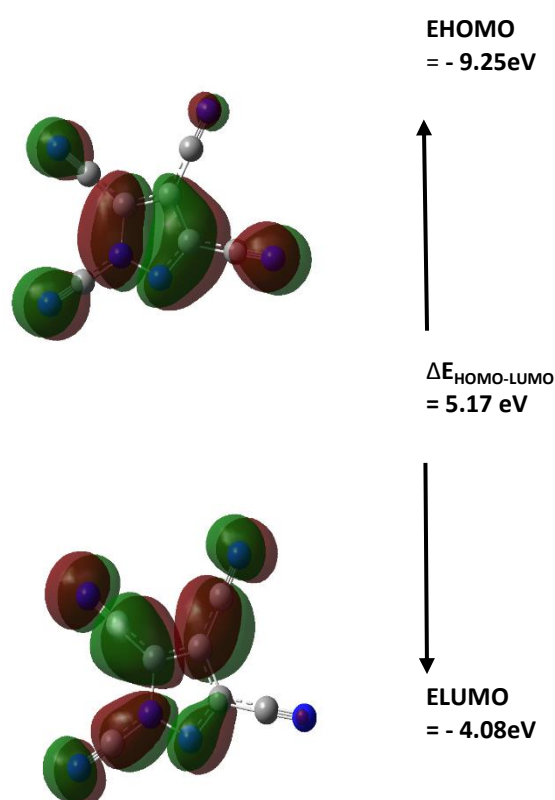


Figure 6: Schematic drawings of the HOMO and LUMO of compound A15

Study of Structure-Activity/Property Relationships for pyrazole Derivatives:

An important objective for this project was to evaluate the physicochemical domain of the fifteen pyrazole derivatives (Figure 8) reported in literature has a biological activity [42]. Some of physicochemical properties were calculated using HyperChem 8.03 software like (Surface Area, Volume, Polarizability, Refractivity and Hydration Energy) and others were calculated using Molinspiration online database (HBA, HBD, TPSA and rotb) For example, (Figure 7) shows the favored conformation in 3D of the compound 2. We will continue this work in the future by a quantitative calculation.

Molecular volume determines transport characteristics of molecules, such as intestinal absorption or blood-brain barrier penetration. Volume is therefore often used in QSAR studies to model molecular properties and biological activity.

The molar refractivity is a steric parameter that is dependent on the spatial array of the aromatic ring in the synthesized compounds. The spatial arrangement also is necessary to study the interaction of the ligand with the receptor [43]. Molar refractivity is related, not only to the volume of the molecules but also to the London dispersive forces that act in the drug receptor interaction.

Molecular Polarizability of a molecule characterizes the capability of its electronic system to be distorted by the external field, and it plays an important role in modeling many molecular properties and biological activities [44]. Solvent-accessible surface bounded molecular volume and van der Waals surface bounded molecular volume calculations are based on a grid method derived by Bodor et al.[45], using the atomic radii of Gavezzotti[46].

Hydration energy is a key factor determining the stability of different molecular conformations in water solutions [47]. The calculation is based on exposed surface area as computed by the approximate method (above), weighted by atom type.

Total polar surface area (TPSA) is a very useful parameter for prediction of drug transport properties. Polar surface area is defined as a sum of surfaces of polar atoms (usually oxygens, nitrogens and attached hydrogens) in a molecule. This parameter has been shown to correlate very well with the human intestinal absorption, Caco-2 monolayer's permeability, and blood-brain barrier penetration [48]. Molecules with PSA values of 140 \AA^2 or more are expected to exhibit poor intestinal absorption [49]. TPSA was used to calculate the percentage of absorption (%ABS) according to the equation: $\%ABS = 109 \pm 0.345 \times TPSA$, as reported [38]. Number of rotatable bonds (nrotb) is a simple topological parameter that measures molecular flexibility and is considered to be a good descriptor of oral bioavailability of drugs [50]. Rotatable bond is defined as any single non-ring bond, bounded to nonterminal heavy (i.e., non-hydrogen) atom. Amide C-N bonds are not considered because of their high rotational energy barrier.

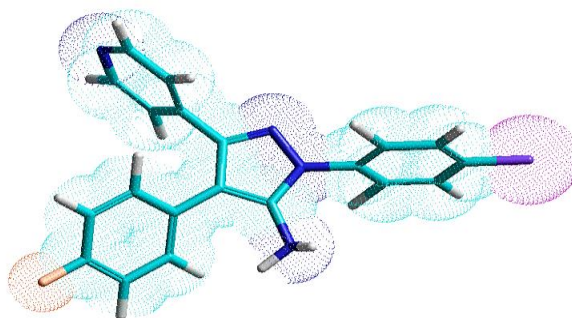


Figure 7: 3D Conformation of compound 2 (HyperChem 8.03)

Structure Property Relationships

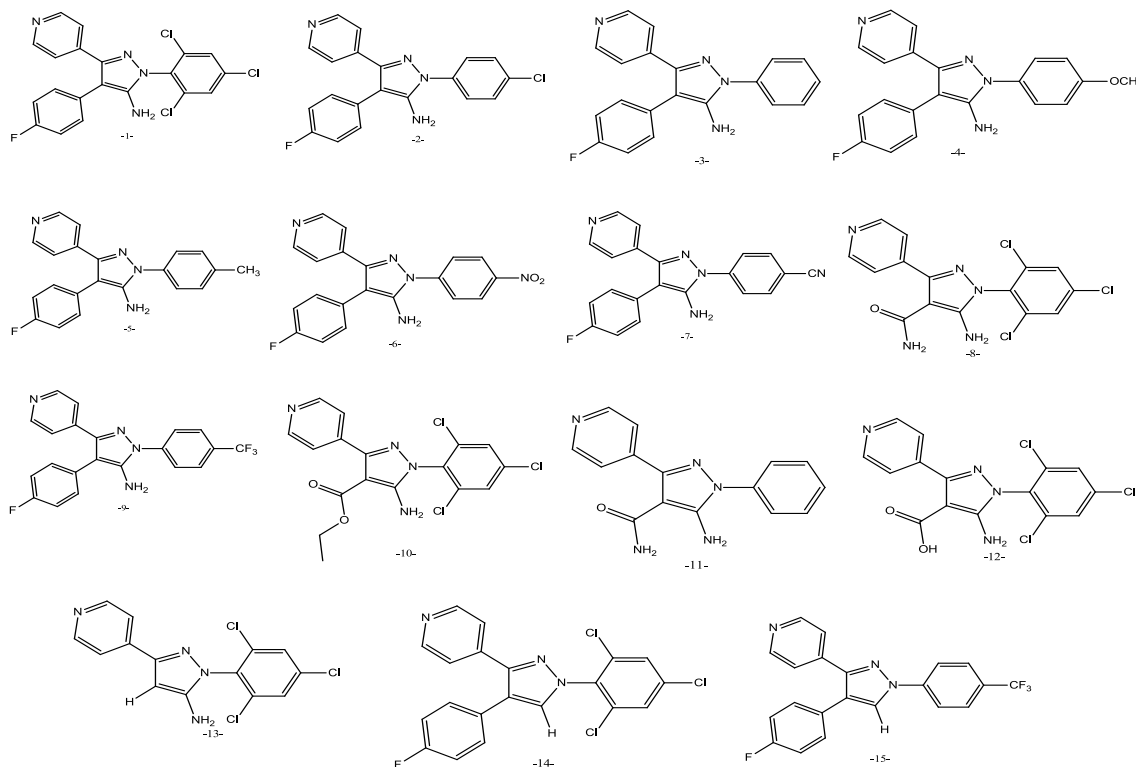


Figure 8: Structural comparison of the pyrazole derivatives

Polarizability values are generally proportional to the values of surfaces and of volumes, the decreasing order of polarizability for these studied pyrazole derivatives is: 1 > 14 > 4 > 10 > 2 > 7 > 5 > 6 > 9 > 15 > 3 > 8 > 12 > 13 > 11 [Table 4].

The order of polarizability is approximately the same one for volume and surface. This also is explained by the relation between polarizability and volume, for the relativity non polar molecules. They are directly linked, for the centers of gravity of negative and positive charges in the absence of external fields to coincide, and the dipole moment of the molecule is zero. For these pyrazole derivatives, surfaces vary from 499.85 Å² to 619.27 Å². These pyrazole derivatives have a great variation of distribution volume, in particular compound 1 and compound 14 which have respective volumes: 1059.49 and 1026.54 Å³ [Table 4].

The most important hydration energy in the absolute value, is that of the compound 6 (14.50 kcal/mol) and the weakest is that of compound 14 (5.20 kcal/mol) [Table 4]. Indeed, in the biological environments the polar molecules are surrounded by water molecules. They are established hydrogen bonds between a water molecule and these molecules. The donor sites of the proton interact with the oxygen atom of water and the acceptor sites of the proton interact with the hydrogen atom (Figure 9).

The first corresponds to the complex with the strongest hydrogen bond. These hydrated molecules are dehydrated at least partially before and at the time of their interaction. These interactions of weak energy, which we observe in particular between messengers and receivers, are generally reversible [51].

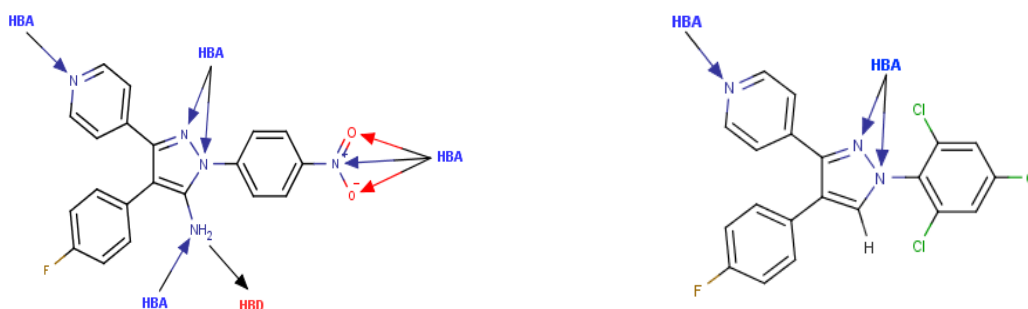


Figure 9: Donor and acceptor sites of compound 6 & compound 14

TPSA of pyrazole derivatives were found in the range of 30.72 - 102.56 and is well below the 140 Å², and we can be observed obviously that all the title compounds (1–15) exhibited a great %ABS ranging from 73.62 % to 98,40%, indicating that these compounds should have good cellular plasmatic membrane permeability [Table 4].

All the screened compounds were flexible, especially, compound 10 which has 5 rotatable bonds.

Table 4. QSAR proprieties for pyrazole derivatives								
Compounds	Surface Area Å ²	Volume Å ³	HE Kcal/mol	Refractivity Å ³	Polazability Å ³	nrotb	TPSA	%ABS
1	619.27	1059.49	-7.20	120.93	42.91	3	56.74	89,42
2	581.58	982.53	-8.34	111.49	39.06	3	56.74	89,42
3	556.92	939.80	-8.69	106.78	37.13	3	56.74	89,42
4	601.46	1016.69	-10.35	113.15	39.60	4	65.97	86,24
5	588.80	991.42	-7.49	111.06	38.96	3	56.74	89,42
6	594.35	1000.07	-14.50	113.00	38.84	4	102.56	73,62
7	594.30	996.21	-12.84	111.76	38.98	3	80.53	81,22
8	554.23	924.85	-11.84	100.10	36.62	3	99.83	74,56
9	601.98	1016.46	-8.06	111.99	38.69	2	56.74	89,42
10	610.20	1026.40	-6.88	107.80	39.57	5	83.05	80,35
11	499.85	815.26	-13.02	85.96	30.83	3	99.83	74,56
12	547.66	915.94	-10.06	98.28	35.90	4	94.04	76,56
13	519.73	851.35	-8.24	92.21	33.34	2	56.74	89,42
14	606.63	1026.54	-5.20	117.94	41.56	3	30.72	98,40
15	591.15	991.08	-5.77	109.00	37.34	4	30.72	98,40

Calculation of drug-likeness properties and lipophilic efficiency (LipE):

Structures of all the selected pyrazole derivatives (Figure 8) were drawn by using ACD labs ChemsSketch v12.0 and their SMILES notations were generated. Smiles notations of the selected compounds were fed in the online Molinspiration software version (www.molinspiration.com) for calculation of molecular properties (number of hydrogen bond donors and acceptors, TPSA and nrotb) [Table 4].

Drug-likeness appears as a promising paradigm to encode the balance among the molecular properties of a compound that influences its pharmacodynamics and pharmacokinetics and ultimately optimizes their absorption, distribution, metabolism and excretion (ADME) in human body like a drug [52]. These parameters allow to ascertain oral absorption or membrane permeability that occurs when the evaluated molecule follows Lipinski's rule of five [molecular weight (MW) \leq 500 Da, $\log P \leq 5$, H-bond donors (HBD) ≤ 5 and H-bond acceptors (HBA) ≤ 10]. Molecules violating more than one of these parameters may have problems with bioavailability and high probability of failure to display drug-likeness [53,54].

However, there are some exceptions to this rule and a compound is likely to be orally active as long as it did not break more than one of his rules because some of orally active drugs such as atorvastatin, cyclosporin do not obey the rule of five.

Octanol/water partition coefficient (LogP) are widely used to make estimation for membrane penetration and permeability, including gastrointestinal absorption [55,56], blood-brain barrier (BBB) crossing, [57,58] and correlations to pharmacokinetic properties [59]. Log P values of pyrazole derivatives were found to be in the range of (-1.46) –(1.29).

Compound 8 is expected to have the highest hydrophilicity because its log P value, whereas compound number 15 and 9 will be the most lipophilic. This implies that these compounds will have poor permeability across cell membrane. Some structural modifications should be carried out to improve their oral absorption, bioavailability and permeability. Low molecular weight drug molecules (<500) are easily transported, diffuse and absorbed as compared to heavy molecules.

Number of hydrogen bond acceptors (O and N atoms) and number of hydrogen bond donors (NH and OH). These quantities have been shown to be critical in a drug development setting as they influence absorption and permeation [60] in the tested compounds were found to be within Lipinski's limit i.e. less than 10 and 5 respectively. The calculation results show that all compounds meet the Lipinski rules of the five, suggesting that these compounds theoretically would not have problems with oral bioavailability.

Table 5: lipophilic efficiency and Lipinski's rule of five for drug likeliness of pyrazole derivatives

Compounds	pIC50	LipE	Log P	MW	nON	nOHNH	n/violations
1	7.47	7,45	0.02	433.70	4	2	0
2	5.62	5,15	0.47	364.81	4	2	0
3	5.92	5,23	0.69	330.36	4	2	0
4	5.72	6,02	-0.30	360.39	5	2	0
5	5.85	5,01	0.84	344.39	4	2	0
6	5.58	5,71	-0.12	375.36	7	2	0
7	5.88	5,48	0.41	355.37	5	2	0
8	5.62	7,08	-1.46	382.64	6	4	0
9	4.51	3,25	1.26	398.36	4	2	0
10	4.00	4,22	-0.22	411.67	6	2	0
11	4.32	5,12	-0.80	279.30	6	4	0
12	4.37	4,97	-0.60	383.62	6	3	0
13	4.06	4,17	-0.11	339.61	4	2	0
14	6.68	6,63	0.05	418.68	3	0	0
15	4.57	3,28	1.29	383.35	3	0	0

^apIC50= -log IC50 , IC50 Anticancer activities

^bLipE = pIC50 – cLogP, ^c calculated by HyperChem program

LipE is an imperative parameter to normalize potency relative to lipophilicity. LipE is used to compare compounds of different potencies (pIC50) and lipophilicities (LogP). For a given compound lipophilic efficiency is defined as the pIC50 (or pEC50) of interest minus the Log P of the compound [61,62].

Although in vitro potency and lipophilicity of compounds are important parameters to evaluate, the concept of Lipophilic Efficiency (LipE) aids in establishing a more balanced relationship between the potency observed in vitro and lipophilicity properties of evaluated chemical compounds [63]. Ryckmans et al. [64] reported that high quality lead compounds possess higher LipE values. We can see through the results in [table 5] that compound 1 had the highest LipE value (7.45) of the data set and was deemed to be the most optimal compound.

CONCLUSION

The present work studied the molecular properties of pyrazole. The PM3 and DFT methods can be used quite satisfactorily in predicting the chemical reactivity of the molecules and the effect of substitution of either donor or acceptor electron.

The compound A11 and A15 have smaller HOMO- LUMO energy gap than others, thus, this compound is the most reactive, and also compound 15 has higher ionization energy (I), higher electron affinity (A), smaller global hardness (η), higher global softness (S), and higher global electrophilicity index (Ω) thus, compound 15 is a strong electrophile than others compounds.

Also, it has smallest HOMO- LUMO energy gap which facilitates intramolecular charge transfer (ICT). The pyrazole derivatives exhibited a great %ABS, which indicating that these compounds should have good cellular plasmatic membrane permeability. And, all these derivatives were flexible, especially, compound 10 which have 5 rotatable bonds.

All compounds meet the Lipinski rules of the five, suggesting that these compounds theoretically would not have problems with oral bioavailability. The compound 1 had the highest LipE value of the data set and was deemed to be the most optimal compound.

REFERENCES

- [1] Brown AC, Fraser TR. *J Anat Physiol* 1868;2(2):224–42.
- [2] Belaidi S, Harkati D, Boughdiri S, Belkhiri L. *Res J Pharm Biol Chem Sci* 2013; 4 (3):1220 – 1234.
- [3] Belaidi S, Mazri R, Mellaoui M, Kerassa A and Belaidi H. *Res J Pharm Biol Chem Sci* 2014; 5(3): 811-818.
- [4] Belaidi S, Bouchlaleg L, Harkati D and Salah T. *Res J Pharm Biol Chem Sci* 2015; 6(2):861-873.
- [5] Sachan A K, Pathak S K, Prasad O, Belaidi S and Sinha L. *Spectrochimica Acta Part A Molecular and Biomolecular Spectroscopy* 2014; 132: 568-581.
- [6] Esposito EX, Hopfinger AJ, Madura JD. *Methods Mol Biol* 2004;275:131–214.
- [7] Dua R, Shrivastava S, Sonwane S K, and Srivastava S K. *J Advan Biol Res* 2011; 5: 120.
- [8] Pimerova E V, Voronina E V. *Pharm Chem J* 2001; 35: 18-20.
- [9] Janus S L, Magdif A Z, Erik B P, Claus N. *Chem* 1999; 130: 1167-1174.
- [10] Park H J, Lee K, Park S, Ahn B, Lee J C, Cho H Y, Lee K I. *Bioorg Med Chem Lett* 2005; 15: 3307-3312.
- [11] Bouabdallah I, M'barek L A, Zyad A, Ramadan A, Zidane I, Melhaoui A. *Nat Prod Res* 2006; 20: 1024-1030.
- [12] Yildirim I, Ozdemir N, Akçamur Y, Dinçer M, Andaç O. *Acta Cryst* 2005; E61: 256-258.
- [13] Bailey D M, Hansen P E, Hlavac A G, Baizman E R, Pearl J, Defelice A F, Feigenson M E. *J Med Chem* 1985; 28: 256-260.
- [14] Chu C K, Cutler J. *J. Heterocycl. Chem* 1986; 23: 289-319.
- [15] Melkemi N, Belaidi S, Salah T and Daoud I. *Res J Pharm Biol Chem Sci* 2015; 6(2): 2017-2024.
- [16] Melkemi N and Belaidi S. *Journal of Computational and Theoretical Nanoscience* 2014; 11: 801-806.
- [17] Abu Thaher B, Arnsmann M, Totzke F, Ehlert J E, Kubbutat M H G, Schachtele C, Zimmermann M O, Koch P, Boeckler F M, and Laufer S A J. *Med Chem* 2012; 55: 961–965.
- [18] Almi Z, Belaidi S and Segueni L. *Rev Theor Sci* 2015; 3: 264-272.

- [19] Salah T, Belaidi S, Melkemi N, Tchouar N. *Rev Theor Sci* 2015; 3: 355-364.
- [20] Belaidi S, Almi Z, Zand Bouzidi D. *Journal of Computational and Theoretical Nanoscience* 2014; 11: 2481-2488.
- [21] Almi Z, Belaidi S, Melkemi N, Boughdiri S, Belkhiri L. *Quantum Matter* 2015; 4.
- [22] Paul S, Mytelka D, Dunwiddie D, Persinger C, Munos B, Lindborg S, Schacht A. *Nat. Rev. Drug Discov.* 2010; 9: 203-14.
- [23] HyperChem (Molecular Modeling System) Hypercube, Inc. USA, 2007.
- [24] M. J. Frisch, G. W. Trucks, H. B. Schlegel, G. E. Scuseria, M. A. Robb, J. R. Cheeseman, G. Scalmani, V. Barone, B. Mennucci, G. A. Petersson, H. Nakatsuji, M. Caricato, X. Li, H. P. Hratchian, A. F. Izmaylov, J. Bloino, G. Zheng, J. L. Sonnenberg, M. Hada, M. Ehara, K. Toyota, R. Fukuda, J. Hasegawa, M. Ishida, T. Nakajima, Y. Honda, O. Kitao, H. Nakai, T. Vreven, J. A. Montgomery, J. E. Peralta, F. Ogliaro, M. Bearpark, J. J. Heyd, E. Brothers, K. N. Kudin, V. N. Staroverov, R. Kobayashi, J. Normand, K. Raghavachari, A. Rendell, J. C. Burant, S. S. Iyengar, J. Tomasi, M. Cossi, N. Rega, J. M. Millam, M. Klene, J. E. Knox, J. B. Cross, V. Bakken, C. Adamo, J. Jaramillo, R. Gomperts, R. E. Stratmann, O. Yazyev, A. J. Austin, R. Cammi, C. Pomelli, J. W. Ochterski, R. L. Martin, K. Morokuma, V. G. Zakrzewski, G. A. Voth, P. Salvador, J. J. Dannenberg, S. Dapprich, A. D. Daniels, J. B. Farkas, Foresman, J. V. Ortiz, J. Cioslowski, and D. J. Fox, Wallingford, CT (2009).
- [25] Database, [<http://www.molinspiration.com>].
- [26] Fantucci P and Valentini V. *J Chem Soc Dalton Trans* 1992; 1981-1988.
- [27] Ramondo F, Tanzi L, Competella M, Gontrani L, Mancini G, Pieretti A and Sadun C. *Phys Chem* 2009; 11: 9431-9439.
- [28] Sidir I, Sidir Y G, Kumalar M, Tasal E. *J Mol Struct* 2010; 964: 134-138.
- [29] Balachandran V, Parimala K. *Spectrochim Acta A* 2012; 96: 340-351.
- [30] Lakshmi A, Balachandran V. *J Mol Struct* 2013; 1033: 40-50.
- [31] Ramalingama S, Karabacak M, Periandy S, Puviarasan N and Tanuja D. *Spectrochim Acta A* 2012; 96: 207-212.
- [32] Mulliken R S. *J. Chem Phys* 1955; 23: 1833-1840.
- [33] Onkar P, Leena S, and Kumar N. *J At Mol Sci* 2010; 1: 201.
- [34] Chunzhi A, Li C Y, Yonghua W, Yadong C, and Ling Y. *J. Bioorg Med Chem Lett* 2009; 19: 803.
- [35] Rajesh K S and Narayan V. *J. Chemical and Pharmaceutical Research* 2012; 4: 3287.
- [36] Pathak J and Sinha L. *J. At Mol Sci* 2012; 3: 95.
- [37] Seminario J M. *Recent Developments and Applications of Modern Density Functional Theory*, Elsevier, Amsterdam, 1996.
- [38] Fleming I. *Frontier Orbitals and Organic Chemical Reactions*, Wiley, New York 1976.
- [39] Koopmans T A. *Physica* 1993; 1: 104-113.
- [40] Parr R J, Szentpaly L V. and Liu S. *J Am Chem Soc* 1999; 121: 1922-1924.
- [41] Parr R J and Pearson R G. *J Am Chem Soc* 1983; 105: 7512-7516.
- [42] Abu Thaher B, Arnsmann M, Totzke F, Ehlert J E, Kubbutat M H G, Schachtele C, Zimmermann M O, Koch P, Boeckler F M, and Laufer S A. *J Med Chem* 2012; 55: 961-965.
- [43] Pankaj P, Kapupara C R, Matholiya A S, Dedakiya, Tusharbindu R D. *Int Bull Drug Res* 2011; 1(1): 1.
- [44] Wang J, Xie X Q, Hou T and Xu X. *Fast J Phys Chem A* 2007; 24 (111): 4443-4448.
- [45] Bodor N, Gabanyi Z and Wpng C K. *J Am Chem Soc* 1989; 111: 3783-3786.
- [46] Gavezzotti A. *J Am Chem Soc* 1983; 105: 5220-5225.
- [47] Ooi T, Oobatake M, Némethy G and Scheraga H A. 1987; 84: 3086-3090.
- [48] Ertl P, Rohde B and Selzer P. *J Med Chem* 2000; 43: 3714-3717.
- [49] Viswanadhan V N, Ghose A K, Revankar G R and Robins R K. *J Chem Inf Comput* 1989; 29: 163-172.
- [50] Veber D F, Johnson S R, Cheng H Y, Smith B R, Ward K W and Kopple K D. *J Med Chem* 2002; 45: 2615-2623.
- [51] Kier L B, *Molecular Orbital Theory in Drug Research*; Academic Press, New York: NY, USA. 1981.
- [52] Vistoli G, Pedretti A and B. Testa 2008; (7-8): 285-294.
- [53] Lipinski C A, Lombardo F, Dominy B W and Feeny P J. *Adv Drug Deliv Rev* 1997; 23: 3-25.
- [54] L. F. Supercomputing Facility for Bioinformatics & Computational Biology-IIT Delhi. L. F. Available from: <http://www.scfbio-iitd.res.in>.
- [55] Winiwarter S, Bonham N M, Ax F, Hallberg A, Lennerna H and Karlen A. *J Med Chem* 1998; 41: 4939-4949.
- [56] Artursson P and Karlsson J. *Biochem. Biophys. Res. Commun.* 1991; 175: 880-885.

- [57] Young R C, Mitchell R C, Brown T H, Ganellin, Griffiths R, Jones M, Rana K, Saunders D, Smith I R, Sore N E and Wilks T J. *J. Med. Chem.* 1988;31: 656–671.
- [58] Waterbeemd H V, Camenisch G, Folkers G, Chretien J R and Raevsky O A. *J Drug Target* 1998;2: 151–165.
- [59] Smith D A, Jones B C and Walker D K. *Med Res Rev* 1996; 16: 243–266.
- [60] Bemis G W and Murcko M A. *J Med Chem* 1996; 39: 2887-2993.
- [61] Edwards M P and Price D A. *Annu Rep Med Chem* 2010; 45: 381–391.
- [62] Leeson PD and Springthorpe B. *Nat Rev Drug Discov* 2007; 6: 881–890.
- [63] Tarcsay A, Nyíri K and Keseru G. *J Med Chem* 2012; 55: 1252–1260.
- [64] Ryckmans T, Edwards M P, Horne V A, Correia A M, Owen D R, Thompson L R, Tran I, Tutt M F and Young T. *Bioorg Med Chem Lett* 2009;19: 4406–4409.